ACS APPLIED MATERIALS & INTERFACES

Letter

www.acsami.org

Gold Nanowire Bundles Grown Radially Outward from Silicon Micropillars

Youju Huang,[†,‡] Abdul Rahim Ferhan,[†] Seok-Jin Cho,[§] Haiwon Lee,[§] and Dong-Hwan Kim*[,†,∥]

[†]School of Chemical and Biomedical Engineering, Nanyang Technological University, 637457, Singapore

[‡]Division of Polymer and Composite Materials, Ningbo Institute of Materials Technology and Engineering, Chinese Academy of Sciences, Ningbo 315201, P. R. China

[§]Department of Chemistry, Hanyang University, Seoul 133-791, Republic of Korea

[∥]School of Chemical Engineering, Sungkyunkwan University, Suwon 16419, Republic of Korea

Supporting Information

ABSTRACT: One-dimensional (1D) micro- and nanostructures have become increasingly popular because of their tremendous prospect in various applications. While the design and fabrication of these structures from a single component in two-dimensional (2D) arrays is common, the attainment of hierarchical three-dimensional (3D) architectures made up of multicomponent one-dimensional structures is rare. Herein we report, for the first time, the lateral growth of gold nanowires from the sidewalls of substrate grown silicon micropillars to form a unique "wire-on-pillar" architecture. Unlike zero-dimensional (0D) point-like, 1D linear, and 2D planar Au structures, the obtained 3D "wire-on-pillar" Au architecture provides abundant hotspots between adjacent Au wires, which led to remarkably high surface-enhanced Raman scattering (SERS) signals.

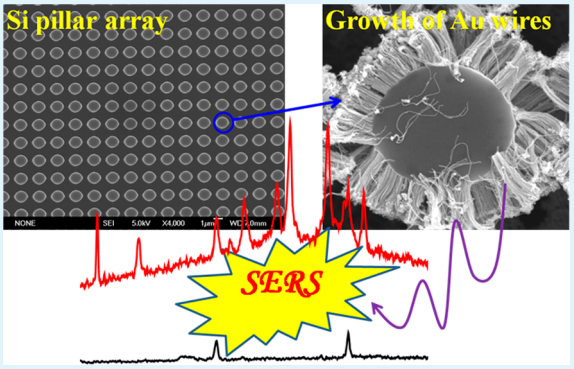

KEYWORDS: *hierarchical nanostructures, gold nanowires, silicon nanowire arrays, SERS substrates, ultrasensitive detection*

There has been an increasing amount of interest in one-dimensional micro- and nanostructures over recent years.[1] These structures, which include free-standing micro- and nanowires as well as vertically grown micro- and nanopillars extending from a substrate surface, have been found to be useful in various applications including solar cells,[2] charge storage devices,[3] vertical transistors,[4] drug delivery systems,[5] and sensors.[6] They are also thought to pave the way for miniaturized devices.[7]

For example, arrays of silicon micropillars have been used to enhance surface capacitance by more than 100% compared to a flat surface of the same area.[8] In addition, when metal-coated, they can also serve as freestanding three-dimensional electrode arrays in microchannels.[9] When hollow silicon dioxide micropillars are coated with several layers of polyelectrolyte, they can be used as pH-triggered drug delivery carriers.[5] Gold nanopillars and nanowires have been used as neural interfaces,[10] and platinum nanowire electrode arrays as biosensors for the detection of glucose from whole blood.[6] The use of other materials such as polymers to form one-dimensional structures has also been demonstrated. For example, Maboudian and co-workers have used polyethyelene micropillar arrays as adhesives.[11]

Despite the vast advantages of one-dimensional structures from complex to simple applications, most reported works have often limited their scope to attaining these structures from a single material component, and in a single orientation such as extending from the substrate surface in the y direction (i.e., vertically oriented) or grown along the xy plane (i.e., horizontally oriented). An inspiring report by Sun and co-workers demonstrated the ability to obtain large area controllable three-dimensional microarchitectures by simply varying the height, shape, width and arrangement of micropillar arrays.[12] Their method served as an alternative to conventional strategies that rely on a combination of top down/bottom up technology. Nonetheless, although this work highlighted the evolution of one-dimensional structures into complex architectures, the structures still comprise a single component.

Because of the immeasurable prospect of one-dimensional micro- and nanostructures, we explore the feasibility of obtaining higher order, three-dimensional multicomponent structures made up of one-dimensional building blocks of different materials grown in different orientations. One fascinating prospect of such 3D structures lies in its application as a 3D plasmonic hotspot matrix, which can be employed for the enhancement of SERS signals. Most reported SERS hotspots exist in 0D point-like, 1D linear, or 2D planar geometries, in which the density of these hotspots is ultimately

Received: June 11, 2015
Accepted: July 23, 2015
Published: July 23, 2015

DOI: 10.1021/acsami.5b05161
ACS Appl. Mater. Interfaces 2015, 7, 17582−17586

limited by zero-, one-, or two-dimensional planes. Here, we grow gold nanowires radially outward, from silicon micropillars to form a unique "wire-on-pillar" superstructure. This was easily constructed based on site-selective growth of Au seeds deposited on the sidewalls of the silicon micropillars. The obtained 3D "wire-on-pillar" Au architecture served well as a novel 3D hotspot matrix, hosting a large number of hotspots between every two adjacent particles in 3D space. This led to remarkable SERS enhancement of R6G probe molecule; around 2 orders of magnitude higher than that obtained from pure Si pillar array. The attainment of these types of structures are expected to pave the way for more complex hierarchical structures, which could further enhance current advantages or even introduce new functionalities.

As we use 4-mercaptobenzoic acid (MBA) as the shape-controlling ligand to achieve one-dimensional growth, we began by studying the effect of MBA concentration variation on the growth of Au nanowires from Au nanoparticle seeds deposited on a flat surface. Silicon wafer was used as the substrate and was first treated with oxygen plasma to improve its surface hydrophilicity. This facilitates the subsequent formation of aminopropyltriethoxysilane (APTES) monolayer, which introduces positive charges on the substrate surface. Because Au nanoparticle seeds are prepared using the citrate-mediated reduction approach,[13−15] the negatively charged citrate-capped seeds can be easily deposited on the substrate surface. Varying the immersion time of the silicon wafer in the Au nanoparticle solution optimizes the assembly density. At optimal density, the concentration of MBA is then varied to see its effect on the Au nanowire growth. We found that MBA concentration (Figure 1) plays an important role in determining the final morphology

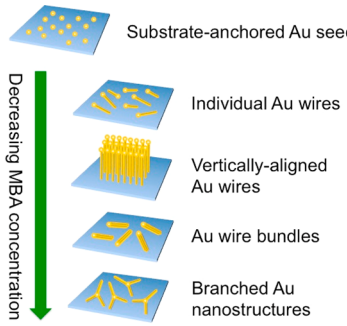

Figure 1. Schematic illustration of shape controlled synthesis of Au nanostructures by substrate-anchored seed-mediated growth.

of Au structures. Since the exposed surfaces of Au seeds were covered by adsorbed MBA molecules, Au atoms can only be deposited at the Au−Si substrate interfaces during the growth of Au wires; the interactions between MBA molecules adsorbed on adjacent Au seeds therefore regulate the self-assembly of formed Au wires. This eventually resulted in radically different structures ranging from loose wires to short spikes when MBA concentration is gradually reduced (Figure 2). Briefly, at MBA concentration of 1 mM, the seeds are almost entirely covered by adsorbed MBA molecules. This hampered access of Au atoms for longitudinal growth. As a result, only thin loose wires grow from the limited exposed sites. These nanowires are randomly dispersed on the substrate in a lying down orientation since 1) not all Au seeds can serve as active growing points and 2) they are not structurally strong enough to support a standing orientation (Figure 2a and Figure S1).

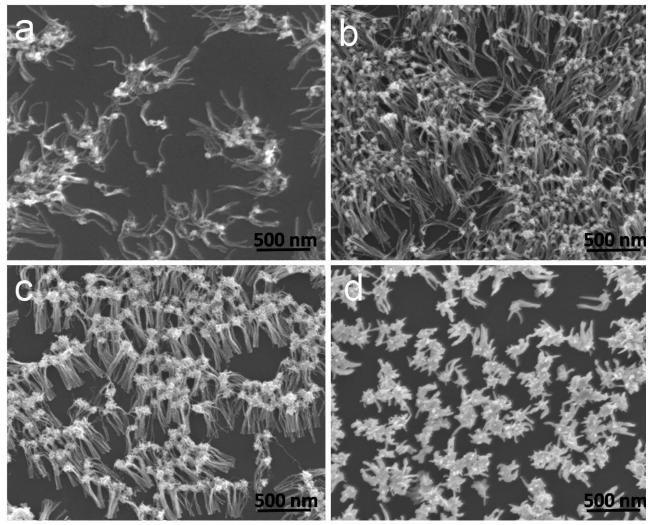

Figure 2. SEM images of Au nanostructures by using substrate-anchored seed mediated growth at different concentrations of MBA ((a) 1 mM, (b) 500 μM, (c) 200 μM, (d) 10 μM).

Interestingly, by slightly reducing the MBA concentration by half, longitudinal growth of Au seeds can be optimized and vertically aligned Au nanowires can be obtained (Figure 2b and Figure S2). By further reducing the concentration to 200 μM, vertical Au nanowires are arranged as bundles (Figure 2c and Figure S3). We believe that at this concentration of MBA, a delicate balance of chemical interactions is reached, which allowed Au seeds to cluster and eventually grow into Au nanowire bundles. To prove the delicateness of this interaction, we then used an MBA concentration of only 10 μM. This disturbed the delicate balance of interactions between MBA molecules. As a result, we could clearly see large Au seed clusters that extend out laterally to form stunted branches giving the impression of short spiky structures (Figure 2d and Figure S4). In addition, the width of Au wires also depended on MBA concentration. When the MBA concentration was reduced from 1000 to 500 and 200 μM, their average diameter increased from 6 to 13, and then 17 nm. We believe that the reduction in MBA allowed more circumferential surface area, especially around the underside (i.e., near the substrate), to be exposed for Au atom attachment during growth. In summary, we can briefly conclude that as MBA concentration is reduced, and MBA coverage on Au seeds becomes sparser, there will be an increasing preference for lateral over vertical growth.

We then used the conditions that favor the formation of Au nanowire bundles to grow Au nanowires radially outward from the sidewalls of Si pillars. A Si pillar array was prepared according to our previous work. The diameter, height and interpillar spacing were set at 1, 3, and 1 μm, respectively. SEM images of the array show the pillars having uniform height and diameter (Figure 3). We also observed that the top surfaces are smoother than the sidewalls.

We then treated the array in a similar fashion as the Si wafer; starting with oxygen plasma treatment, followed by APTES modification, Au seed deposition and finally the growth of Au nanowire bundles. Interestingly, we found that nanowire density, locality and orientation all varied interdependently by changing the growth duration.

When the growth time was 5 min, minimal growth occurred at the top surface. Instead, thick and long nanowire bundles were seen to grow near the top, but out of the sidewalls, when

DOI: 10.1021/acsami.5b05161
ACS Appl. Mater. Interfaces 2015, 7, 17582−17586

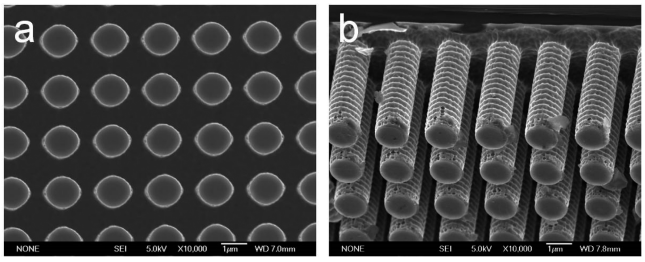

Figure 3. SEM images of Si pillar array ((a) top view, (b) tilted view at 60° tilt angle).

the growth time was increased to 15 min. Furthermore, nanowires growing out from adjacent pillars have the tendency to fuse, resulting in the formation of a network of interpillar bridge-like structures (Figure 4b, b′). Interestingly, the fused structures only connect the pillars at 90° angles; there is no such structure between diagonally neighboring pillars. This can be accounted by the length of the Au wires, which is around 550 nm, allowing them to fuse only across the smallest interpillar distance of 1 μm (i.e., at 90° angles). Only when the growth time was further increased to 30 min could we start to see the radially outward growth of Au nanowire bundles (Figure 4c, c′). Although the bundles were thick, there were still gaps at some regions around the sidewalls of the Si pillars, indicating incomplete growth. Complete growth occurred after 60 min, resulting in complete coverage of the top regions of the sidewalls with Au nanowire bundles (Figure 4d, d′). The final structure resembles a wire-on-pillar umbrella with Si pillar as the shaft and Au nanowire bundles as the canopy (Figure S5). The reason for the formation of the umbrella-shaped structure can be broken down into two parts. First, the smooth surface at the top of the Si surface may hamper the growth of Au nanowires due lower chemical activity. Second, Au nanowires only grow out of the top region of the Si pillar sidewalls since Au seeds may have difficulty being deposited around the lower region in the first place. Consequently, it would be difficult for Au nanowires to grow in this region.

We believe our hierarchical structures are most well suited for surface-enhanced Raman scattering (SERS) applications. SERS is a powerful analytic technique that have been used to detect molecular targets in various fields including biology,[16] chemistry,[17] medicine,[18] food safety,[19] environment,[20] etc. To enhance SERS signals, we have systematically investigated nanoparticles of different shapes, sizes, compositions, and uniformity. Theoretical and experimental studies[21,22] revealed that sharp metallic protrusions and nanogaps could significantly enhance SERS signals by up to 2−3 orders of magnitude. These regions of extreme enhancements are referred as "hotspots". A simple way of obtaining hotspots is through the dense assembly of gold or silver nanoparticles on a surface, which would yield an abundant number of gaps between adjacent nanoparticles. Recently, many groups have taken one step further by either depositing the nanoparticles in a three-dimensional fashion[23−25] or on Si nanowires[26] in an attempt to further increase the hotspot density. Although such structures of the latter can, similar to our case, be considered as multicomponent, they are essentially nanoparticle-decorated Si nanowires. In contrast, our Au wire-on-pillar structures are not only three-dimensional in nature, they are also hierachically arranged to produce junctions that interconnect adjacent pillars over a large scale, which would serve as an entirely novel type of SERS hotspot.

Rhodamine 6G (R6G) was used as the probe molecule for the SERS measurement (Figure 5). We studied SERS signals

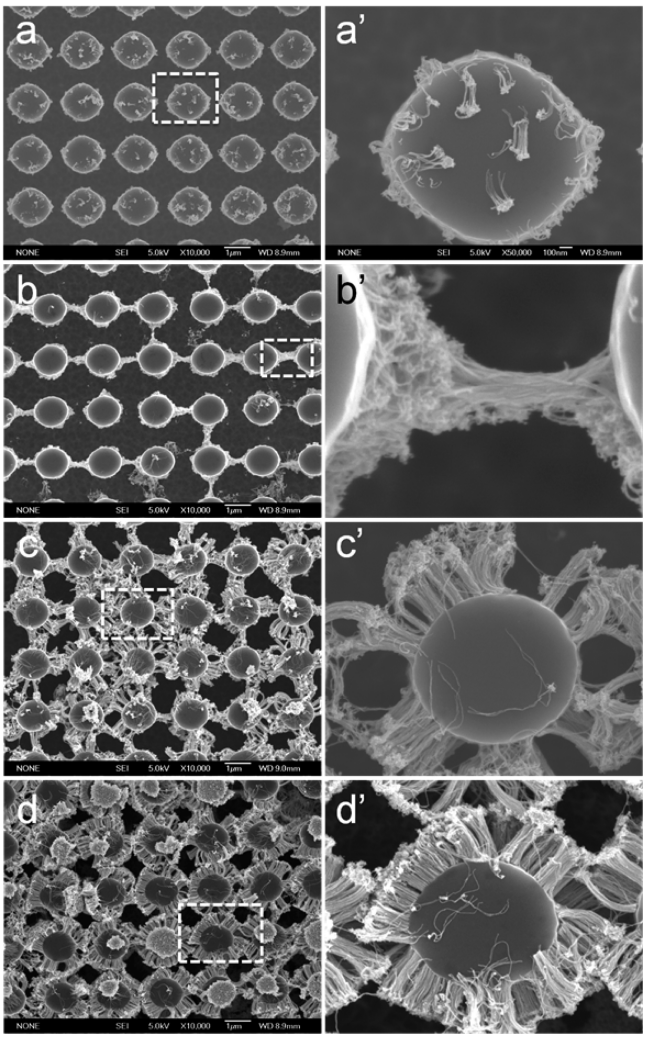

Figure 4. SEM images of Au wires bundles decorated Si pillar array at different growth times ((a) 5, (b) 15, (c) 30, and (d) 60 min) and (a′−d′) their corresponding SEM images with low magnification.

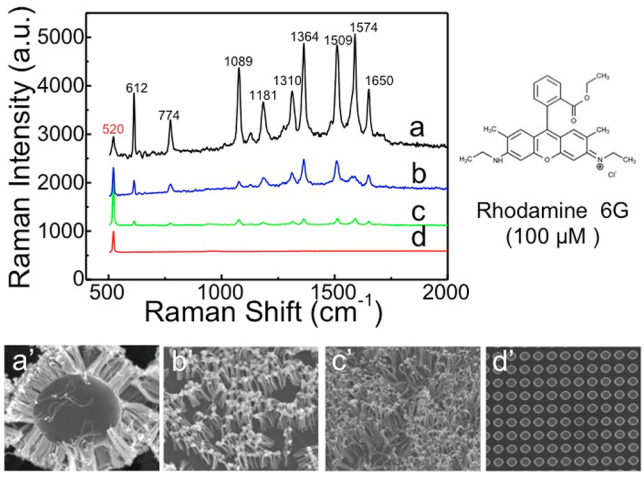

Figure 5. SERS spectra a-d of R6G obtained from Au nanosctructures (SEM images a′−d′), respectively. The spectra were obtained with λ_{ex} = 632.8 nm excitation.

DOI: 10.1021/acsami.5b05161
ACS Appl. Mater. Interfaces 2015, 7, 17582−17586

from four representative samples − (1) Au wire-on-pillar umbrella structure (Figure 5a′), (2) Au nanowire bundles (Figure 5b′), (3) loose Au nanowires (Figure 5c′), and (4) as-prepared Si pillars without any Au structure (Figure 5d′). All of these structures are supported on Si substrates each measuring 0.5 × 0.5 cm^2. R6G was dissolved in ethanol (0.1 mM) and 5 μL of the solution was dropped on the different substrates before obtaining the signals using a 633 nm HeNe laser source with one accumulation and 10s exposure time. Undoubtedly, SERS signal intensities from sample 1 (Figure 5a) shows largest enhancement compared to the other samples, with a R6G limit of detection of 10 μM (Figure 5b−d). The SERS enhancement performance of the substrate can quantified according to previous works.[21,27,28] The averaged enhancement factors (EF) were calculated by taking the 520 cm^{-1} peak as the reference and by comparing R6G signals from bare silicon. Averaged EFs of approximately 8.6 × 10^6, 1.4 × 10^6, and 6.4 × 10^5 were obtained for samples (1), (2), and (3), respectively. Because SERS enhancement not only depends on the inherent structures of Au nanoparticles (e.g., sharp tips and valleys) but also on the density of "hotspots" between adjacent Au nanoparticles, the high density of "hotspots" arising from adjacent Au wires arranged in bundles plays an important role in SERS signal enhancement. Furthermore, the wire-on-pillar umbrella structures covered almost the entire substrate, providing maximum "hotspot" density for SERS enhancement compared to lateral arrangement of gold nanowire bundles. In addition, the wire-on-pillar umbrella structure can also easily capture SERS molecules compared to lateral gold nanowire bundles, which would indirectly improve SERS enhancement.

In summary, we have reported the lateral, radially outward growth of Au nanowire bundles from the sidewalls of Si pillars to form a unique wire-on-pillar structure resembling an umbrella. While we have so far demonstrated the advantage of this structure as a SERS platform, which is promising for sensing and optical imaging applications, we believe that the novelty of the structure can be further exploited in other applications like solar cells, electrode arrays, and charge storage devices.

■ ASSOCIATED CONTENT

Supporting Information

The Supporting Information is available free of charge on the ACS Publications website at DOI: 10.1021/acsami.5b05161.

Detailed experimental procedures for the preparation of gold seeds and gold nanowires as well as all supporting figures (PDF)

■ AUTHOR INFORMATION

Corresponding Author

*E-mail: dhkim1@skku.edu.

Author Contributions

The manuscript was written through contributions of all authors. All authors have given approval to the final version of the manuscript.

Notes

The authors declare no competing financial interest.

■ ACKNOWLEDGMENTS

We gratefully acknowledge the financial support of the Ministry of Science, ICT & Future Planning of Korea (NRF-2013M3C8A3078512), the Natural Science Foundation of China (21404110 and 51473179), and Defense Acquisition Program Administration and Agency for Defense Development (UD140080GD).

■ REFERENCES

(1) Xia, Y.; Yang, P.; Sun, Y.; Wu, Y.; Mayers, B.; Gates, B.; Yin, Y.; Kim, F.; Yan, H. One-Dimensional Nanostructures: Synthesis, Characterization, and Applications. *Adv. Mater.* **2003**, *15*, 353−389.

(2) Zhang, Y.; Diao, Y.; Lee, H.; Mirabito, T. J.; Johnson, R. W.; Puodziukynaite, E.; John, J.; Carter, K. R.; Emrick, T.; Mannsfeld, S. C. B.; Briseno, A. L. Intrinsic and Extrinsic Parameters for Controlling the Growth of Organic Single-Crystalline Nanopillars in Photovoltaics. *Nano Lett.* **2014**, *14*, 5547−5554.

(3) Zou, X.; Liu, X.; Wang, C.; Jiang, Y.; Wang, Y.; Xiao, X.; Ho, J. C.; Li, J.; Jiang, C.; Xiong, Q.; Liao, L. Controllable Electrical Properties of Metal-Doped In2o3 Nanowires for High-Performance Enhancement-Mode Transistors. *ACS Nano* **2012**, *7*, 804−810.

(4) Tomioka, K.; Yoshimura, M.; Fukui, T. A Iii-V Nanowire Channel on Silicon for High-Performance Vertical Transistors. *Nature* **2012**, *488*, 189−192.

(5) Alba, M.; Formentin, P.; Ferre-Borrull, J.; Pallares, J.; Marsal, L. Ph-Responsive Drug Delivery System Based on Hollow Silicon Dioxide Micropillars Coated with Polyelectrolyte Multilayers. *Nanoscale Res. Lett.* **2014**, *9*, 411.

(6) Yang, M.; Qu, F.; Lu, Y.; He, Y.; Shen, G.; Yu, R. Platinum Nanowire Nanoelectrode Array for the Fabrication of Biosensors. *Biomaterials* **2006**, *27*, 5944−5950.

(7) Garcia-Frutos, E. M. Small Organic Single-Crystalline One-Dimensional Micro- and Nanostructures for Miniaturized Devices. *J. Mater. Chem. C* **2013**, *1*, 3633−3645.

(8) Ya'akobovitz, A.; Hart, A. J. Enhanced Surface Capacitance of Cylindrical Micropillar Arrays. *Sens. Actuators, A* **2014**, *219*, 32−37.

(9) Kilchenmann, S. C.; Rollo, E.; Bianchi, E.; Guiducci, C. Metal-Coated Silicon Micropillars for Freestanding 3d-Electrode Arrays in Microchannels. *Sens. Actuators, B* **2013**, *185*, 713−719.

(10) Nick, C.; Quednau, S.; Sarwar, R.; Schlaak, H. F.; Thielemann, C. High Aspect Ratio Gold Nanopillars on Microelectrodes for Neural Interfaces. *Microsyst. Technol.* **2014**, *20*, 1849−1857.

(11) Kim, Y.; Chung, Y.; Tsao, A.; Maboudian, R. Tuning Micropillar Tapering for Optimal Friction Performance of Thermoplastic Gecko-Inspired Adhesive. *ACS Appl. Mater. Interfaces* **2014**, *6*, 6936−6943.

(12) Wu, D.; Wu, S.-Z.; Zhao, S.; Yao, J.; Wang, J.-N.; Chen, Q.-D.; Sun, H.-B. Rapid, Controllable Fabrication of Regular Complex Microarchitectures by Capillary Assembly of Micropillars and Their Application in Selectively Trapping/Releasing Microparticles. *Small* **2013**, *9*, 760−767.

(13) Huang, Y.; Kim, D.-H. Synthesis and Self-Assembly of Highly Monodispersed Quasispherical Gold Nanoparticles. *Langmuir* **2011**, *27*, 13861−13867.

(14) Zhang, L.; Dai, L.; Rong, Y.; Liu, Z.; Tong, D.; Huang, Y.; Chen, T. Light-Triggered Reversible Self-Assembly of Gold Nanoparticle Oligomers for Tunable Sers. *Langmuir* **2015**, *31*, 1164−1171.

(15) Zhang, L.; Huang, Y.; Wang, J.; Rong, Y.; Lai, W.; Zhang, J.; Chen, T. Hierarchical Flowerlike Gold Nanoparticles Labeled Immunochromatography Test Strip for Highly Sensitive Detection of Escherichia Coli O157:H7. *Langmuir* **2015**, *31*, 5537−5544.

(16) Kong, X.; Yu, Q.; Zhang, X.; Du, X.; Gong, H.; Jiang, H. Synthesis and Application of Surface Enhanced Raman Scattering (Sers) Tags of Ag@Sio2 Core/Shell Nanoparticles in Protein Detection. *J. Mater. Chem.* **2012**, *22*, 7767−7774.

(17) Zhang, P.; Sui, Y.; Wang, C.; Wang, Y.; Cui, G.; Wang, C.; Liu, B.; Zou, B. A One-Step Green Route to Synthesize Copper Nanocrystals and Their Applications in Catalysis and Surface Enhanced Raman Scattering. *Nanoscale* **2014**, *6*, 5343−5350.

(18) Wang, H.; Jiang, X.; Wang, X.; Wei, X.; Zhu, Y.; Sun, B.; Su, Y.; He, S.; He, Y. Hairpin DNA-Assisted Silicon/Silver-Based Surface-Enhanced Raman Scattering Sensing Platform for Ultrahighly Sensitive

DOI: 10.1021/acsami.5b05161
ACS Appl. Mater. Interfaces 2015, 7, 17582−17586

and Specific Discrimination of Deafness Mutations in a Real System. *Anal. Chem.* **2014**, *86*, 7368−7376.
(19) Zhang, Y.; Yu, W.; Pei, L.; Lai, K.; Rasco, B. A.; Huang, Y. Rapid Analysis of Malachite Green and Leucomalachite Green in Fish Muscles with Surface-Enhanced Resonance Raman Scattering. *Food Chem.* **2015**, *169*, 80−84.
(20) Zhang, K.; Ji, J.; Li, Y.; Liu, B. Interfacial Self-Assembled Functional Nanoparticle Array: A Facile Surface-Enhanced Raman Scattering Sensor for Specific Detection of Trace Analytes. *Anal. Chem.* **2014**, *86*, 6660−6665.
(21) Fang, Y.; Seong, N.-H.; Dlott, D. D. Measurement of the Distribution of Site Enhancements in Surface-Enhanced Raman Scattering. *Science* **2008**, *321*, 388−392.
(22) Li, W.; Camargo, P. H. C.; Lu, X.; Xia, Y. Dimers of Silver Nanospheres: Facile Synthesis and Their Use as Hot Spots for Surface-Enhanced Raman Scattering. *Nano Lett.* **2008**, *9*, 485−490.
(23) Han, Z.; Liu, H.; Wang, B.; Weng, S.; Yang, L.; Liu, J. Three-Dimensional Surface-Enhanced Raman Scattering Hotspots in Spherical Colloidal Superstructure for Identification and Detection of Drugs in Human Urine. *Anal. Chem.* **2015**, *87*, 4821−4828.
(24) Liu, H.; Yang, Z.; Meng, L.; Sun, Y.; Wang, J.; Yang, L.; Liu, J.; Tian, Z. Three-Dimensional and Time-Ordered Surface-Enhanced Raman Scattering Hotspot Matrix. *J. Am. Chem. Soc.* **2014**, *136*, 5332−5341.
(25) Sun, Y.; Han, Z.; Liu, H.; He, S.; Yang, L.; Liu, J. Three-Dimensional Hotspots in Evaporating Nanoparticle Sols for Ultrahigh Raman Scattering: Solid-Liquid Interface Effects. *Nanoscale* **2015**, *7*, 6619−6626.
(26) Wang, H.; Han, X.; Ou, X.; Lee, C.-S.; Zhang, X.; Lee, S.-T. Silicon Nanowire Based Single-Molecule Sers Sensor. *Nanoscale* **2013**, *5*, 8172−8176.
(27) Huang, Y.; Dandapat, A.; Kim, D.-H. Covalently Capped Seed-Mediated Growth: A Unique Approach toward Hierarchical Growth of Gold Nanocrystals. *Nanoscale* **2014**, *6*, 6478−6481.
(28) Huang, Y.; Kim, D.-H. Light-Controlled Synthesis of Gold Nanoparticles Using a Rigid, Photoresponsive Surfactant. *Nanoscale* **2012**, *4*, 6312−6317.

DOI: 10.1021/acsami.5b05161
ACS Appl. Mater. Interfaces 2015, 7, 17582−17586